



## ***Characterization and origin of episyenites in the southern Caballo Mountains, Sierra County, NM***

V.T. McLemore, A. Smith, A.M. Riggins, Dunbar N., K.B. Frempong, and M.T. Heizler

2018, pp. 207-216. <https://doi.org/10.56577/FFC-69.207>

Supplemental data: <https://nmgs.nmt.edu/repository/index.cfm?rid=2018006>

in:  
*Las Cruces Country III*, Mack, Greg H.; Hampton, Brian A.; Ramos, Frank C.; Witcher, James C.; Ulmer-Scholle, Dana S., New Mexico Geological Society 69<sup>th</sup> Annual Fall Field Conference Guidebook, 218 p.  
<https://doi.org/10.56577/FFC-69>

---

*This is one of many related papers that were included in the 2018 NMGS Fall Field Conference Guidebook.*

---

## **Annual NMGS Fall Field Conference Guidebooks**

Every fall since 1950, the New Mexico Geological Society (NMGS) has held an annual [Fall Field Conference](#) that explores some region of New Mexico (or surrounding states). Always well attended, these conferences provide a guidebook to participants. Besides detailed road logs, the guidebooks contain many well written, edited, and peer-reviewed geoscience papers. These books have set the national standard for geologic guidebooks and are an essential geologic reference for anyone working in or around New Mexico.

### **Free Downloads**

NMGS has decided to make peer-reviewed papers from our Fall Field Conference guidebooks available for free download. This is in keeping with our mission of promoting interest, research, and cooperation regarding geology in New Mexico. However, guidebook sales represent a significant proportion of our operating budget. Therefore, only *research papers* are available for download. *Road logs*, *mini-papers*, and other selected content are available only in print for recent guidebooks.

### **Copyright Information**

Publications of the New Mexico Geological Society, printed and electronic, are protected by the copyright laws of the United States. No material from the NMGS website, or printed and electronic publications, may be reprinted or redistributed without NMGS permission. Contact us for permission to reprint portions of any of our publications.

One printed copy of any materials from the NMGS website or our print and electronic publications may be made for individual use without our permission. Teachers and students may make unlimited copies for educational use. Any other use of these materials requires explicit permission.

*This page is intentionally left blank to maintain order of facing pages.*

# CHARACTERIZATION AND ORIGIN OF EPISYENITES IN THE SOUTHERN CABALLO MOUNTAINS, SIERRA COUNTY, NEW MEXICO

VIRGINIA T. McLEMORE<sup>1</sup>, ADAM SMITH<sup>1</sup>, ANNEISE M. RIGGINS<sup>2</sup>, NELIA DUNBAR<sup>1</sup>, KWAME BOAFO  
FREMPONG<sup>1</sup>, AND MATTHEW T. HEIZLER<sup>1</sup>

<sup>1</sup>New Mexico Bureau of Geology and Mineral Resources, New Mexico Institute of Mining and Technology, Socorro, NM, 87801; [virginia.mcmore@nmt.edu](mailto:virginia.mcmore@nmt.edu)

<sup>2</sup>Los Alamos National Laboratory, Los Alamos, New Mexico

**ABSTRACT**—Brick-red, K-feldspar-rich rocks, called episyenites (altered rocks that were desilicated and metasomatized by alkali-rich solutions) are found in several areas in southern and central New Mexico. These rocks contain anomalous concentrations of rare earth elements (REE, <2329 ppm), uranium (U, <9721 ppm), thorium (Th, <1378 ppm), niobium (Nb, <247 ppm) and high heavy REE (<133 ppm Yb and <179 ppm Dy). In the Caballo Mountains, the timing of metasomatism is older than late Cambrian as episyenite clasts occur in the Cambrian-Ordovician Bliss Formation that unconformably overlies episyenites and Proterozoic host rocks. <sup>40</sup>Ar/<sup>39</sup>Ar dating of K-feldspars within the episyenites yields complex and intriguing age results that are likely related to multiple fluid-alteration events possibly during the Ancestral Rocky Mountains and Laramide orogenies. Rare U, Th, Nb, and REE minerals are found in the Caballo episyenites and could indicate potential REE mineralization at depth, including heavy REE. Synchronite is a major host of light REEs in the episyenites, while heavy REEs are concentrated predominantly in xenotime and priorite. Textural evidence and field relationships indicates that REE-bearing phases co-precipitated during metasomatism prior to deposition of the Cambrian-Ordovician Bliss Formation. The maximum age of the metasomatism forming the episyenites is between the age of the host granite (~1400 Ma) and the Bliss Formation (late Cambrian-early Ordovician). The K-feldspars in the episyenites were then re-heated during the Ancestral Rocky Mountains and Laramide orogenies.

## INTRODUCTION

Brick-red, K-feldspar-rich rocks, called episyenites, were first found in southern New Mexico in the 1950s during exploration for uranium deposits (Fig. 1; Staatz, et al., 1965; McLemore, 1986). Some of these complexes in New Mexico and elsewhere are known for potential economic deposits of rare earth elements (REE), uranium (U), thorium (Th), niobium (Nb), and other elements (Long et al., 2010; McLemore, 2015). Rare earth elements (REE) and other critical elements are increasingly becoming more important in our technological society. Because of the chemical and physical properties of REE, they are used in many diverse defense, energy, industrial, and military applications, like cell phones, computers, magnets, batteries, solar panels, and wind turbines (Long et al., 2010). Because of this importance, the authors mapped and sampled these unusual metasomatic rocks, with the goals of better understanding their tectonic setting, mechanisms of origin, and to evaluate their economic potential. Similar episyenites and fenites are found elsewhere in New Mexico and southern Colorado (Fig. 1) and are thought to be part of a Cambrian-Ordovician alkaline magmatic event that is documented throughout southern Colorado and New Mexico (Armbrustmacher, 1984; McMillan and McLemore, 2004; Riggins et al., 2014; McLemore, 2016; McLemore and Lueth, 2017). However, new age dating of the Caballo episyenites yields complex and intriguing age results that are likely related to multiple fluid-alteration events of different ages, and there is no geochronological evidence to support a relationship to the Cambrian-Ordovician alkaline magmatic event in the Caballo Mountain.

## DEFINITION OF EPISYENITES

The term *episyenite* is used to describe altered rocks that were desilicified (subsolvus dissolution of quartz) and metasomatized by alkali-rich fluids (Leroy, 1978; Recio et al., 1997). The metasomatic rocks in several areas in New Mexico, including the Caballo, Burro, and Zuni Mountains, Sevilleta Wildlife Refuge, and Lobo Hill (Fig. 1), were erroneously called syenites and alkali granites (Condie and Budding, 1979; McMillan and McLemore, 2004) but are actually metasomatic in origin and not primary igneous rocks (McLemore, 2013, 2016; Riggins, 2014; Riggins et al., 2014; Smith, 2018). Elsewhere in the world, these alkali-rich metasomatic rocks are associated with uranium and thorium deposits (Costi et al., 2002; Condomines et al., 2007; Cuney et al., 2012), gold deposits (López-Moro et al., 2013) and tin-tungsten deposits (Charoy and Pollard, 1989; Costi et al., 2002; Borges et al., 2009), but many unmineralized episyenites are found as well (Petersson and Eliasson, 1997; Recio et al., 1997; Hecht et al., 1999; Nishimoto et al., 2014). Episyenites are similar to altered rocks formed by fenitization and would be called fenites by some geologists. Fenitization is the alkali-metasomatism associated with carbonatites or alkaline igneous activity (Le Bas, 2008). However, we are reluctant to use the term fenite for these rocks studied here because there is no definitive spatial association with carbonatite or alkaline igneous rocks. Despite numerous studies on episyenites, the origin and mechanism of the formation of these potentially REE-, U-, Th- and Nd-enriched rocks is unknown. This report summarizes results and interpretations of on-going mapping, geochemical, and geochronological studies.

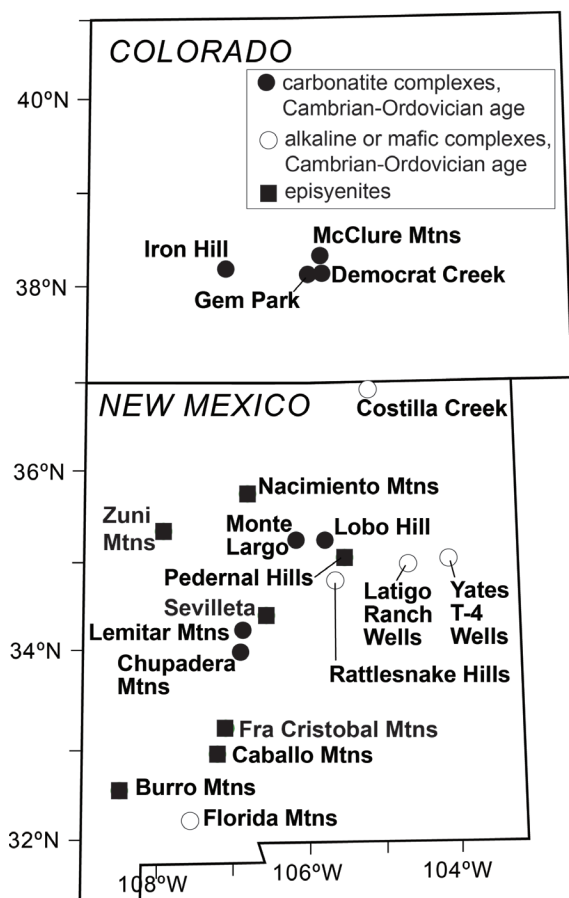


FIGURE 1. Locations of areas with episyenites in New Mexico.

## PREVIOUS WORK

In the 1950s, prospectors located several areas of anomalously high radioactivity in the Caballo Mountains and attributed it to the presence of uranium. Shallow prospect pits and adits were dug and holes drilled on many of the claims in the area (Appendix 1); but, assay results were low and the claims were later dropped with no production. Radioactive syenite dikes were reported in the southern Red Hills in the Caballo Mountains by Melancon (1952) and Boyd and Wolfe (1953) during a reconnaissance for uranium deposits. The radioactive deposits in the southern Red Hills were subsequently studied in more detail by Staatz et al. (1965) and McLemore (1986). In 2012, the New Mexico Bureau of Geology and Mineral Resources (NMBGMR) began more detailed examination of these unusual rocks; Riggins (2014) and Riggins et al. (2014) presented preliminary results of that research. Smith (2018) continued to examine these rocks. Recently, mining claims and surface sampling of some of these bodies have been undertaken by prospectors looking for REE.

## METHODOLOGY

Field investigations of the metamorphic and plutonic rocks in the Caballo Mountains by the senior author began in 1980 in order to assess their economic potential and tectonic setting (McLemore, 1986). Continued examinations occurred in

1995–1996, as part of the evaluation of mineral resources in the Caballo resource area in Sierra and Otero Counties (Green and O'Neill, 1998). In 2012–2017, more detailed investigations were carried out.

Published and unpublished data were compiled and examined. Mineral occurrences, deposits, mines, and prospects were identified, plotted on base maps, described in detail (Appendix 1), and compiled in the New Mexico Mines Database. Detailed field mapping at scales of 1:6,000 to 1:12,000 were compiled in ARCMAP® using U.S. Geological Survey (USGS) topographic maps as the map base (Figs. 2, 3, 4). Color versions of the geologic maps are in Appendix 2 along with color photographs of episyenites. The mapping in 2012–2017 is more accurate than previous mapping because a handheld GPS unit was used with the current topography loaded in the unit.

Selected samples of the Proterozoic host rocks and episyenites were collected and analyzed by a variety of methods. Rock samples collected during 1985 were analyzed for major and trace elements by X-ray fluorescence (XRF) at the NMBGMR XRF laboratory, on a PW 2400 instrument using standard instrument settings on fused glass discs and trace elements using pressed powder briquettes. Mineralized samples collected for the USGS Caballo project in 1995–1996 were submitted to the USGS for analyses by Inductively Coupled Plasma-Atomic Emission Spectrometry (ICP-AES) and INAA. Additional analyses of the igneous and metasomatic rocks collected in 2012–2017 were by XRF and ICP by Activation Laboratories, methods for which can be found at [www.actlabs.com](http://www.actlabs.com). Mineralogy of selected samples was determined by X-ray diffraction (XRD). Locations of samples and whole-rock geochemical analyses are in Appendix 3.

Selected samples of episyenite and granitic host rocks were investigated using a Cameca SX100 electron microprobe at NMBGMR to characterize compositional, chemical and textural characteristics of host granite and episyenite. Episyenite samples chosen for microprobe analysis were selected based on two criteria: 1) elevated whole-rock concentrations of U, Th, and REE, and 2) texture and relationship with the granitic host rock. Samples of granitic host rocks were selected from areas known to have undergone minimal alteration, and are therefore representative of original host rock compositions and textures. More details on the analytical procedures are by Riggins (2014) and Smith (2018).

Selected K-feldspar samples of episyenite were dated by furnace incremental heating  $^{40}\text{Ar}/^{39}\text{Ar}$  age spectrum method by the New Mexico Geochronological Research Laboratory (NMGR) at NMBGMR. Samples of granitic host rock were also dated to provide a baseline of K-feldspar age behavior for the area. Samples were crushed and sieved, and K-feldspars were hand-picked under a binocular microscope. An effort was made to avoid picking K-feldspars that were obviously zoned, contained inclusions, or had attached fragments of other minerals. Grains were washed with deionized water in a sonic bath to remove fine-grained particulates and dried at room temperature, before being loaded into aluminum discs for irradiation. Samples were irradiated at the USGS TRIGA reactor in Denver, CO for 40 hours. Fish Canyon 2 sanidine was used to monitor neu-

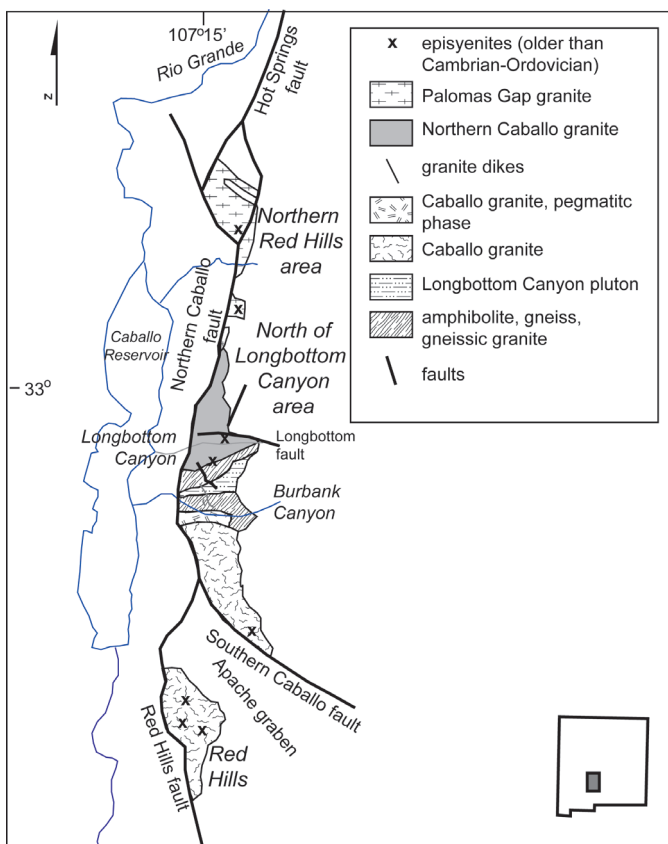


FIGURE 2. Simplified geologic map of Proterozoic rocks and Cambrian-Ordovician episyenites of the Caballo Mountains, New Mexico (modified from Condie and Budding, 1979; Seager and Mack, 2003; McLemore et al., 2012).

tron flux, with an assigned age of 28.204 Ma. After irradiation, single K-feldspar crystals were loaded into copper trays and placed under vacuum. Crystals were step-heated with a 50W CO<sub>2</sub> laser and analyzed by the NMGR Mass Analyzer Products 215-50 mass spectrometer or step-heated with the NMGR sample furnace and analyzed with the Helix MC Plus multicollector mass spectrometer. More detailed laboratory methods are described at <http://geoinfo.nmt.edu/labs/argon/home.html> and in Riggins (2014) and Smith (2018).

## GEOLOGY OF CABALLO MOUNTAINS

The Caballo Mountains are an east-dipping fault block along the eastern Rio Grande Rift in central New Mexico (Fig. 2) and are comprised of rocks ranging in age from Proterozoic to Recent. The Proterozoic rocks in the Caballo Mountains have been mapped by Kelley and Silver (1952), Staatz et al. (1965), Condie and Budding (1979), Bauer and Lozinsky (1986), McLemore (1986), and Seager and Mack (1991, 2003, 2005). Proterozoic plutonic rocks form the lower slopes of the Caballo Mountains and include at least four different granitic bodies (Caballo granite, Longbottom granite/granodiorite pluton, Northern Caballo granite, Palomas Gap pluton) that are intruded by pegmatite, granite, and aplite dikes. Age dates are summarized in Table 1.

The oldest rocks in the Caballo Mountains are ~1680 Ma metamorphosed amphibolites, quartz-feldspathic schist (parag-

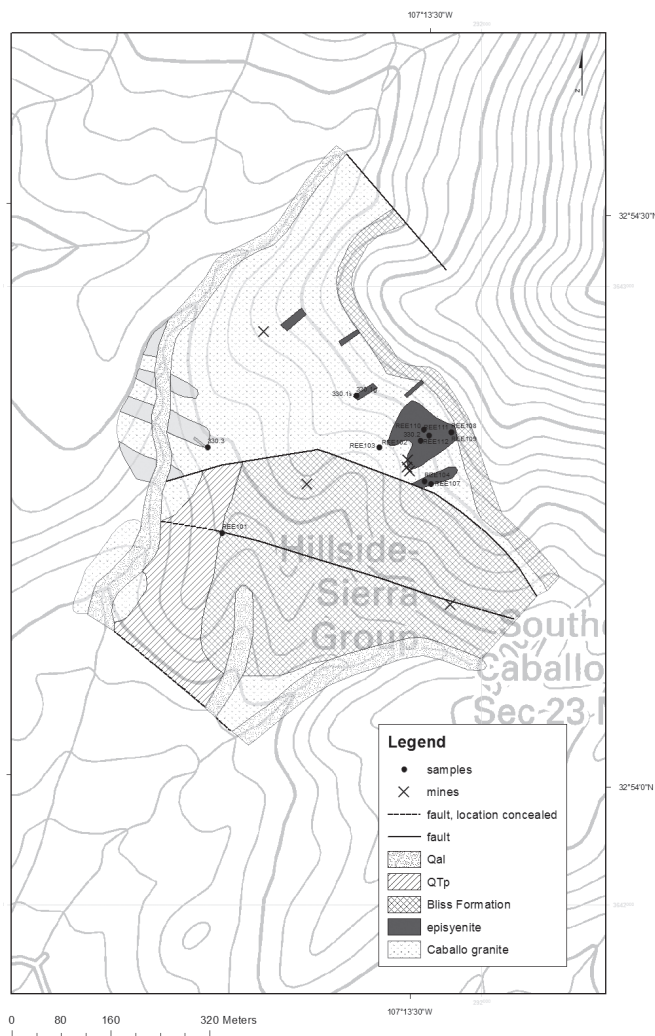


FIGURE 3. Geologic map of the Apache Gap episyenites area, southern Caballo Mountains.

neiss), felsic gneiss, and granitic gneiss (orthogneiss) exposed in the Longbottom and Burbank Canyons (Condie and Budding, 1979; Bauer and Lozinsky, 1986; McLemore, 1986; Seager and Mack, 2003, 2005; Amato and Becker, 2012; McLemore et al., 2012). The ~1486 Ma Longbottom Canyon pluton intruded the metamorphic complex (Seager and Mack, 2003; Amato and Becker, 2012), is concordant with metamorphic foliation, and consists of large euhedral microcline and plagioclase megacrysts (as much as 3 cm long) in a medium-grained matrix of quartz, plagioclase, microcline, biotite, and titanite. The pluton is gray, weathers to tan, and varies in lithology from granodiorite to granite. The pluton contains numerous metamorphic amphibolitic and gneissic xenoliths.

The ~1487 Ma Caballo granite forms the largest exposure of the granitic rocks in the Caballo Mountains and extends from Burbank Canyon, southward into Apache Gap and the Southern Red Hills (Fig. 2; Seager and Mack, 2003; Amato and Becker, 2012; McLemore et al., 2012). The northern portion of the pluton is pegmatitic in texture. The Caballo granite is pink to orange- to buff-colored, medium- to coarse-grained granite consisting of nearly equal amounts of quartz, microcline, and





TABLE 1. Summary of ages of Proterozoic granites and younger episyenites from the Caballo Mountains (UTM coordinates are NAD 27, Zone 13; locations in parenthesis are from Amato and Becker, 2012). Geologic units are defined by Condie and Budding (1979), Seager and Mack (2003), and McLemore et al. (2012). std dev- standard deviation.

Sample	Latitude (decimal degrees)	Longitude (decimal degrees)	Geologic Unit	Description	Integrated $^{40}\text{Ar}/^{39}\text{Ar}$ Age (K-feldspar) Ma (McLemore et al., 2012; Smith, 2018)	Integrated $^{40}\text{Ar}/^{39}\text{Ar}$ Age (biotite) Ma (McLemore et al., 2012; Smith, 2018)	U-Pb ages (Amato and Becker, 2012)
CAB11-7	33.049636	107.230396	Palomas Gap granite	gray to pink granite, with quartz, feldspar	609.1±1.0		
CAB11-4	32.94469	107.254995	granite dike	white granite dike cutting Caballo granite containing quartz, feldspar, biotite	919±1.3	1010.6±1.6	
CAB11-2	32.977427	107.247333	Northern Caballo granite	gray to tan, fine grained granite	1001.2±1.5		
06CM-01	32.943815	107.258513	Caballo granite				1487±24
CAB11-6, 06CM-01	32.959758	107.255506	Longbottom granodiorite/ granite pluton	brown-gray porphyritic granodiorite to granite, large phenocrysts of microcline and plagioclase in a finer-grained matrix of quartz, plagioclase, microcline, biotite	1106.4±1.5	1375.9±1.7	1486±16
06CM-02	32.960427	107.261877	gneissic granite				1681±12
REE-1004	32.880238	107.255502	Caballo granite	equigranular aplite dike of Caballo granite, partially chloritized	1017.8±1.1 (average of 3 analyses)	1354.33±0.64	
REE-1005	32.880238	107.255502	Caballo granite	Coarse grained granite with fully chloritized biotite, small (<1 cm long) megacrysts of K-feldspar, plagioclase and quartz	998.1±3.5 (average of 3 analyses)		
REE-1003	32.876984	107.255901	Episyenite (S. Red Hills)	Nearly completely altered episyenite with brick-red feldspar, chlorite (±vermiculite?) bearing, LREE enriched	404.4±2.6 (std. dev: 37.1) (average of 11 analyses)		
REE-1007	32.880238	107.255502	Episyenite (S. Red Hills)	nearly completely altered episyenite, brick red K-feldspar, contains chlorite and fluorite, xenotime	394.5±2.0 (std. dev: 42.3) (average of 12 analyses)		
REE-1009	32.880238	107.255502	Episyenite (S. Red Hills)	pale pink, partially altered pegmatite, original graphic quartz texture destroyed	417.8±1.0 (std dev: 17.9) (average of 3 analyses)		

3). The episyenites are within the Caballo granite, steeply dipping lens-shaped bodies, and consist of coarse- to fine-grained K-feldspar and lesser amounts of disseminated quartz, hematite, and chlorite. The coarse-grained zones resemble the textures of unaltered pegmatite dikes. One episyenite body is 76 m wide and 123 m long and another body is 91 m long and 46 m wide. Three additional bodies are much smaller. The outcrop patterns are linear, suggesting fracture or fault control. Porous zones of ellipsoidal cavities (vugs) with interstitial coarse-grained K-feldspar and quartz (less than 5 cm wide) are found within the episyenite and could represent fluid pathways, but it is uncertain if the open spaces are a result of dissolution or nondeposition of crystals. These zones locally grade into a breccia of cemented K-feldspar crystals. Within the lenses of episyenite, original amphibolite has been altered to a dark red-brown and greenish-black episyenite. The contacts between

the brick-red episyenite and orange to buff-colored Caballo granite and black amphibolite are generally sharp. Two prospect pits have exposed the episyenites (Appendix 1), but only thin veins of manganese oxides, hematite, and clay are found cutting the episyenite. The episyenite lenses are unconformably overlain by the black to dark brown iron-rich sandstone of the Bliss Formation or are faulted adjacent to the Bliss ironstone or limestone. The overlying Bliss conglomerate locally contains pebbles and smaller fragments of episyenites, mixed with unaltered quartz and K-feldspar and pink granite pebbles and smaller fragments (Appendix 2).

### Southern Red Hills

More than 25 lenticular to elongate pods, lenses (<100 m long, <10 m wide), narrow pipe-like and dike-like bodies (<2 m

wide, 400 m long) of episyenites are found scattered throughout the Southern Red Hills, south of Apache Gap (Appendix 1) and locally form clusters or linear zones, possibly along local fracture or shear zones (Fig. 4). Episyenites are commonly exposed near pegmatite and aplite dikes. Several pits, one quarry, and one adit have exposed many of the episyenites (Appendix 1). Contacts between episyenites and the Caballo granite vary between sharp, irregular, and gradational. Within the episyenites, gradational contacts are characterized by an increase in grain size towards the contact. The episyenites typically consist of microcline (as determined by XRD), with subordinate amounts of quartz, muscovite, hematite/goethite, chlorite, and locally trace plagioclase and other accessory minerals. Some episyenites in the Southern Red Hills contain as much as 95% microcline, whereas other episyenites contain as much as 25% quartz. Some episyenites contain porous zones of ellipsoidal cavities (vugs) with interstitial coarse-grained K-feldspar and quartz (less than 5 cm wide) that could represent fluid pathways, similar to those found at Apache Gap. Many episyenites in the Southern Red Hills contain dark brown-green to brown to black aggregates (as much as 2 cm in diameter) of specular hematite and chlorite (as determined by XRD), with a variety of accessory minerals (Table 2).

MINERALOGY AND PARAGENESIS

Episyenite samples were examined by petrographic microscope and electron microscope to determine textures and mineralogy. Feldspars are subhedral to anhedral, and plagioclase (~25%) and K-feldspar (~35%) are both present. New growth

of feldspar is observed as overgrowth rims and as replacements of pre-existing feldspar in the pre-existing granite from grain boundaries inward. Secondary feldspar is similar to feldspar in fully altered episyenite; i.e. K-rich, lacking exsolution textures, hematite-rich and turbid with fragmentary to subhedral grain boundaries. Most episyenites contain abundant fractured and vuggy K-feldspar with micron sized iron-oxide inclusions. Chlorite and vermiculite forms pseudomorphs after biotite, while the original diamond-shaped form of amphibole is replaced by fine-grained aggregates of chlorite, Fe-oxides, rutile, and possibly calcite. Apatite is euhedral and prismatic, while zircon is usually subhedral, rounded, and displays growth zoning. Calcite is present as late-stage fracture fill and is fine grained and turbid. Oxides are principally hematite, but magnetite and secondary rutile are present as well. Several samples also contain patchy cores of plagioclase and K-feldspar without iron-oxide inclusions surrounded by rims of K-feldspar with iron-oxide inclusions. Iron and titanium oxides are most commonly present in areas of apparent alteration of mafic xenoliths or aggregates of mafic minerals within the original granite. Some relict shapes and textures of primary mafic silicates are preserved. Vugs and fracture fillings contain quartz, and varying amounts of chlorite, apatite, iron and titanium oxides, zircon, calcite, fluorite, magnetite, barite, and U-, Th- and REE-bearing minerals (Table 2). At least three stages of fluorite (dark purple in color) are present in episyenites: an early disseminated fluorite adjacent to K-feldspars, fluorite along thin veinlets cutting K-feldspar, and late-stage fluorite in vugs and along fractures surfaces (Fig. 5). REE-bearing phases are typically associated with areas of altered mafic silicates and include synchysite, thorite, xenotime and uranophane (Fig. 5; Table 2). A few yellowish-brown minerals are also present that are likely monazite. Thorite locally occurs in ring structures and is commonly surrounded by iron-oxide. Episyenite sample REE-148 contains similar sized crystals of synchysite and thorite in contact with one another. The contacts are sharp and display no evident cross-cutting relationships. Synchysite is a major host of light REEs in the episyenites (63 wt.% light REE), while heavy REEs are concentrated predominantly in xenotime (16 wt.% heavy REE) and priorite (9 wt.%). Oxidation of uraninite to kasolite and uranophane is found at the Plainview adit. Uranophane commonly displays a scaly texture, suggesting dehydration. From

TABLE 2. Rare minerals found in the episyenites in the southern Caballo Mountains.

Mineral	Formula	Method of analysis	Comment
Apatite	Ca <sub>5</sub> (PO <sub>4</sub> ) <sub>3</sub> (F,Cl,OH)	Thin section, electron microprobe	
Zircon	ZrSiO <sub>4</sub>	Thin section, electron microprobe	
Monazite	(Ce,Ln)PO <sub>4</sub>	Thin section, electron microprobe	
Rutile	TiO <sub>2</sub>	electron microprobe	
Synchysite	Ca(Ce,Ln)(CO <sub>3</sub> ) <sub>2</sub> F	electron microprobe	
Thorite	(Th,U)SiO <sub>4</sub>	XRD, electron microprobe	
Thorogummite	Th(SiO <sub>4</sub> ) <sub>0.9</sub> (OH) <sub>0.4</sub>	XRD	
Xenotime	YPO <sub>4</sub>	electron microprobe	
Uraninite	UO <sub>2</sub>	XRD	
Uranophane	Ca(UO <sub>2</sub> ) <sub>2</sub> SiO <sub>3</sub> (OH) <sub>2</sub> •5(H <sub>2</sub> O)	electron microprobe, XRD	
Aeschnynite	(Y,Ca,Fe,Th)(Ti,Nb) <sub>2</sub> (O,OH) <sub>6</sub>	electron microprobe	Longbottom Canyon
Priorite	(Y,Ln,Ca,Th)(Ti,Nb) <sub>2</sub> (O,OH) <sub>6</sub>		
Kasolite	Pb(UO <sub>2</sub> ) <sub>2</sub> SiO <sub>4</sub> •H <sub>2</sub> O	XRD	Oxidation product of uraninite
Bastnaesite	Ce(CO <sub>3</sub> )F	XRD	
Symplectite?	Fe <sup>2+</sup> <sub>3</sub> (AsO <sub>4</sub> ) <sub>2</sub> •8H <sub>2</sub> O	XRD	
Uranopilite?	(UO <sub>2</sub> ) <sub>6</sub> (SO <sub>4</sub> )O <sub>2</sub> (OH) <sub>6</sub> •14H <sub>2</sub> O	XRD	
Fluorite	CaF <sub>2</sub>	Visible, XRD	
Crandallite	CaAl <sub>3</sub> (PO <sub>4</sub> )(PO <sub>3</sub> OH)(OH) <sub>6</sub>	electron microprobe	
Pyrochlore	(Na,Ca) <sub>2</sub> Nb <sub>2</sub> O <sub>6</sub> (OH,F)	electron microprobe	
Nb-rutile?	TiO <sub>2</sub>	electron microprobe	



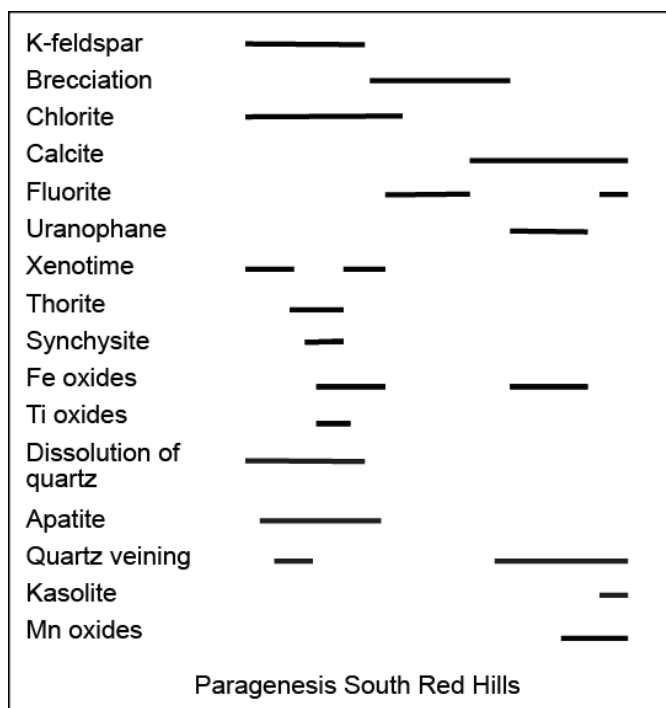


FIGURE 5. Paragenesis of U-Th-REE mineralization in the Southern Red Hills, Caballo Mountains.

these observations a paragenesis of the mineral assemblage was developed (Fig. 5). Table 2 summarizes the rare minerals found in the southern Caballo Mountains.

### WHOLE-ROCK GEOCHEMISTRY

Selected samples of granite and episyenites in the Caballo Mountains were collected and analyzed for major and trace elements (Appendix 3). The Caballo episyenites are higher in  $K_2O$  (as high as 15.33%),  $Al_2O_3$ , Rb and slightly in Ba and lower in  $SiO_2$ , Sr and  $Na_2O$  (<0.4%) than samples of the Caballo granites (Riggins, 2012; Smith, 2018). Some episyenites have similar chondrite-normalized REE patterns (Fig. 6) as the Caballo granites, although other episyenite samples are enriched in REE (<2329 ppm), U (<9721 ppm), Th, (<1378 ppm), Nb (<247 ppm) and heavy REE (<133 ppm Yb and <179 ppm Dy) (Appendix 2). The Caballo episyenites are similar in composition to episyenites found in the Burro and Zuni Mountains, Seville National Wildlife Refuge, and at Lobo Hill (McLemore, 1986, 2016; McLemore and McKee, 1988, 1989; McLemore et al., 1999; McMillan and McLemore, 2004; Riggins, 2014; Riggins et al., 2014).

### DISCUSSION Age of the episyenites

Detailed mapping has shown that episyenites in the Southern Red Hills of the Caballo Mountains are unconformably overlain by the Cambrian–Ordovician Bliss Formation and thus record alteration of Precambrian rocks prior to about ~500 Ma. The basal transgressive conglomerate of the Bliss local-

ly contains clasts of episyenites and granitic clasts adjacent to episyenite clasts in the basal Bliss are not altered (Appendix 2). Riggins (2014) analyzed a sample of the conglomerate on the electron microprobe, and found that the red episyenites grains have sharp, rounded boundaries. This indicates that the clasts are detrital, and were not formed in situ by an alteration or magmatic event. Additionally, several of the episyenites clasts contain xenotime with a similar REE pattern to xenotime from in-place episyenites bodies. This further indicates that episyenites were present in some form prior to the deposition of the Bliss Formation.

However, secondary K-feldspar from the Caballo episyenites yields  $^{40}Ar/^{39}Ar$  ages mostly between ~309 to 437 Ma (Fig. 7; Riggins, 2014; Smith, 2018), which suggests potential crystallization during the Ancestral Rocky Mountain orogeny, and thus too young to directly record the pre-500 Ma metasomatic event. However in the Palomas Gap and Apache Gap areas, much younger ages were recorded from 34–55 Ma and 40–50 Ma, respectively. These were interpreted to record possible thermal resetting during the Laramide orogeny (Riggins, 2014; Smith, 2018). Nearby, unaltered primary K-feldspars from Proterozoic host rocks have  $^{40}Ar/^{39}Ar$  age spectra that rise abruptly from initial ages between 550 and 700 Ma ages to near plateau ages ranging from ~925 to ~1050 Ma, indicating that the late Paleozoic ages of the secondary episyenite K-feldspar are not cooling ages, but rather represent K-feldspar recrystallization associated with low temperature alteration events (Table 1). The presence of numerous types of mineral deposits found in the Caballo Mountains, as described above, suggest that mineralizing fluids could have affected these rocks during the Paleozoic and are supportive of the variance in  $^{40}Ar/^{39}Ar$  ages.

### Formation of episyenites

Textures, high K-feldspar contents, and high  $K_2O$  concentrations support a metasomatic origin of the Caballo episyenites (McLemore, 1986; Riggins, 2014; Smith, 2018). The field and mineralogical observations suggest that the Caballo episyenites were formed by interaction of a K-rich fluid with the granitic host rock, possibly along fault, fracture, and shear zones. The most altered rocks contain more than 15 wt.%  $K_2O$ , which is close to the composition of endmember orthoclase (15.60 wt.%  $K_2O$ ; Deer et al., 1992; Riggins, 2014; Riggins et al., 2014; Smith, 2018), suggesting the most altered rocks are composed almost completely of K-feldspar. The K-rich fluid that caused metasomatism was likely silica undersaturated, resulting in dissolution and/or alteration of primary quartz, biotite and other accessory silicate phases (Cathelineau, 1986), and precipitation of secondary K-feldspar with iron-oxide inclusions. Similar observations are found in the episyenites found in the Seville National Wildlife Refuge and Burro Mountains (Riggins, 2014; Riggins et al., 2014; McLemore, 2016).

One sample of the episyenite in the Burro Mountains yielded  $^{40}Ar/^{39}Ar$  plateau ages of  $516.4 \pm 4.5$  to  $533.3 \pm 5.2$  Ma, which is consistent with formation during the Cambrian–Ordovician (Riggins, 2014). However, other samples from the Caballo and Burro Mountains yields complex and intriguing age results that

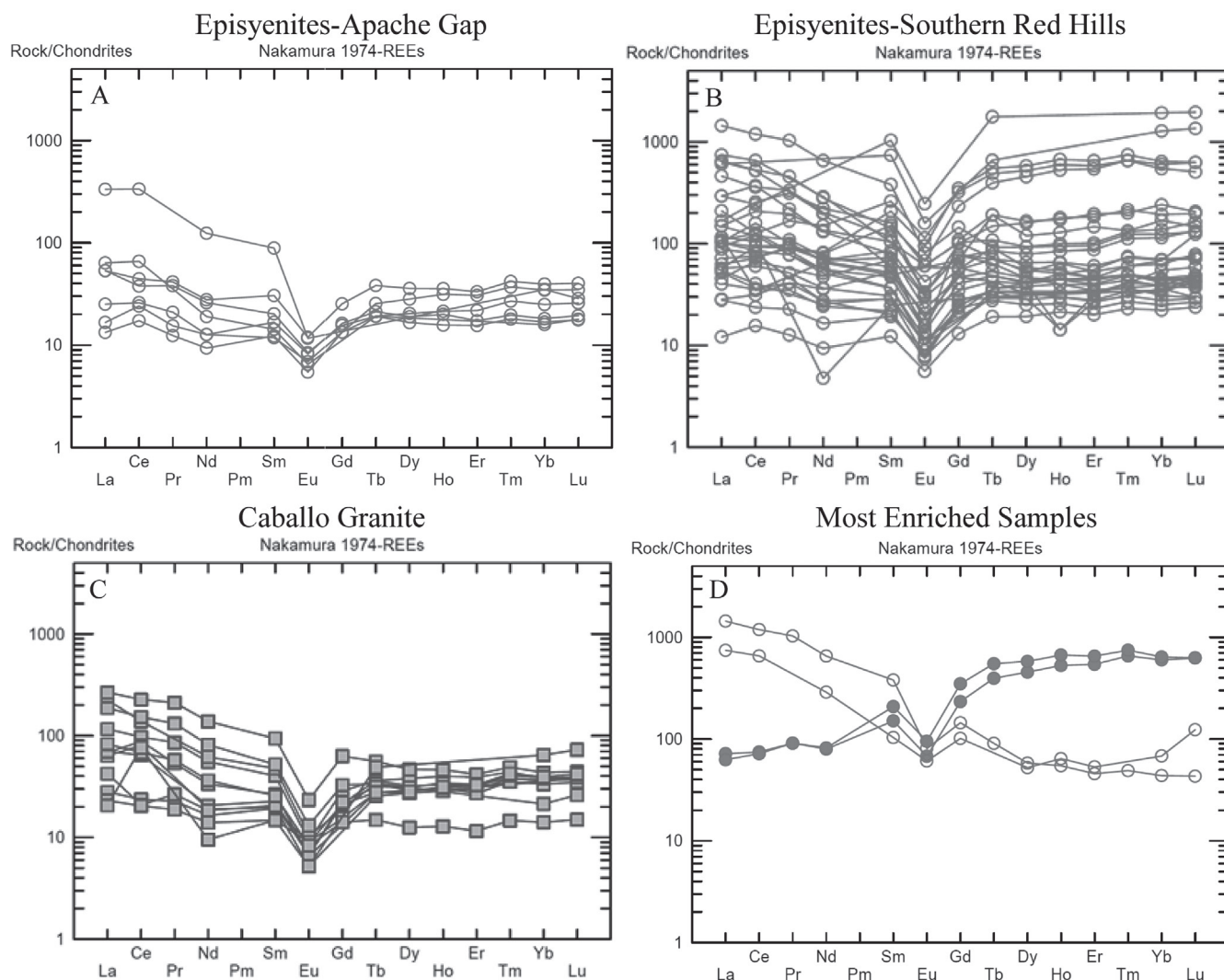


FIGURE 6. Chondrite normalized REE patterns for the Caballo granite and episyenites. Chondrite values from Nakamura (1974). Chemical analyses are in Appendix 3. 6D displays data from the most LREE enriched samples (hollow circles), and most HREE enriched samples (solid circles).

are likely related to multiple alteration events, and therefore cannot constrain the maximum age of episyenite formation (Riggins, 2014; Smith, 2018).  $^{40}\text{Ar}/^{39}\text{Ar}$  ages suggests potential crystallization of new K-feldspar during the Ancestral Rocky Mountain orogeny and additional potential reheating during the Laramide orogeny. Collectively, these data clearly indicate that the Caballo episyenites were formed before ~500 Ma prior to Cambrian–Ordovician Bliss Formation, and subsequently reheated during alteration during the Ancestral Rocky Mountain and Laramide orogenies. Additional age dating is required to constrain the maximum age of episyenites, perhaps with in situ U-Pb dating of the xenotime, uraninite or thorite.

#### MINERAL-RESOURCE POTENTIAL

In general, the exposed outcrops of episyenites in the Caballo Mountains appear too small and low grade to be economic in today's market. There are no carbonatites exposed at the surface in the Caballo Mountains. However, drilling and subsurface sampling are required to fully evaluate the miner-

al-resource potential. The Lobo Hill episyenites near Moriarty are currently being mined for crushed decorative stone, and the Lobo Hill episyenites are approximately 20 m deep and drilling suggests episyenites extends another 20–30 m. Thus episyenites can be extensive in the subsurface. The relatively high HREE in some episyenites in the Caballo Mountains could be of economic interest, but additional mineralogical, geochemical, and economic analyses are required to fully assess the mineral-resource potential.

#### CONCLUSIONS

The episyenites in the southern Caballo Mountains are metasomatic in origin and the maximum age of the metasomatism forming the episyenites is between the age of the host granite (~1400 Ma) and the Cambrian–Ordovician Bliss Formation (~500 Ma). Subsequent metasomatism and recrystallization of K-feldspars occurred during the Ancestral Rocky Mountain and Laramide orogenies. Rare U, Th, Nb and REE minerals are found in the Caballo episyenites and could indi-

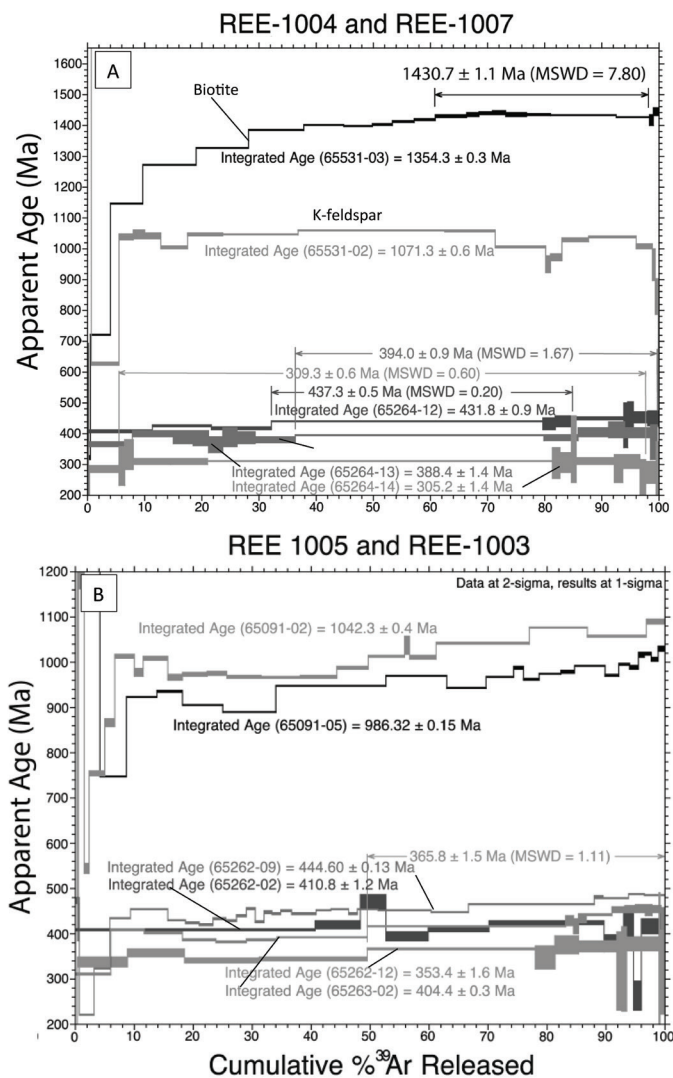


FIGURE 7. Age spectra from samples in the southern Red Hills of the Caballo Mountains. Integrated ages and are shown and for each spectrum and plateaus are identified when valid. **A)** Age spectra from REE-1004 (Caballo granite) and K-feldspar fragments from REE-1007 (fully altered episyenite). From REE-1004, both K-feldspar and biotite were dated. **B)** K-feldspar age spectra of coarse-grained Caballo granite (REE-1005) and the episyenite it hosts (REE-1003). In both cases, crystals from the granite define ages greater than ~800 Ma, while the episyenites define a range of ages from ~300–450 Ma.

cate potential REE mineralization at depth, including heavy REE, which are important economic commodities.

#### ACKNOWLEDGMENTS

This paper is part of an on-going study of the mineral resources of New Mexico at NMBGMR, Dr. Nelia Dunbar, Director and State Geologist. Field mapping and sampling assistance was by James McLemore. Miles L. Silberman (Agricola Minerals LLC) and O. Tapani Rämö (University of Helsinki, Finland) reviewed an earlier version of this manuscript and their comments are appreciated.  $^{40}\text{Ar}/^{39}\text{Ar}$  dating of episyenites and granite samples was carried out by A. Riggins, A. Smith, M. Heizler, L. Peters and W. McIntosh at NMBGMR. XRD analyses were by K. Frempong and A. Smith. Electron mi-

croprobe analysis of episyenites and granite samples was performed by A. Riggins, A. Smith and L. Heizler at NMBGMR. The Cameca SX-100 electron microprobe at NMINT was partially funded by NSF Grant STI-9413900. Partial funding for the XRD Laboratory at the NMBGMR was provided by a grant from the U.S. Department of Education (MAC700). This study was partially financially supported by USGS Mineral Resources External Research Program (award number G12AP20051). NMGS and NMBGMR supported A. Riggins, K. Frempong, and A. Smith. K. Frempong was also supported by the Department of Mineral Engineering at NMINT. A. Riggins and A. Smith would like to thank the NMBGMR Kottowski Graduate Fellowship for additional financial support.

#### REFERENCES

- Amato, J.M. and Becker, T., 2012, Proterozoic rocks of the Caballo Mountains and Kingston mining district: U-Pb geochronology and correlations within the Mazatzal province of Southern New Mexico: New Mexico Geological Society, Guidebook 64, p. 227-234.
- Armbrustmacher, T.J., 1984, Alkaline rock complexes in the Wet Mountains, Custer and Fremont Counties, Colorado: U.S. Geological Survey, Professional Paper 1269, 33 p.
- Bauer, P.W. and Lozinsky, R.P., 1986, Proterozoic geology of supracrustal and granitic rocks in the Caballo Mountains, southern New Mexico: New Mexico Geological, Guidebook 37, p. 143-149.
- Borges, R.M.K., Villas, R.N.N., Fuzikawa, K., Dall'Agnol, R., and Pimenta, M.A., 2009, Phase separation, fluid mixing, and origin of the greisens and potassic episyenites associated with the Água Boa pluton, Pitinga tin province, Amazonian craton, Brazil: *Journal of South American Earth Science*, v. 27, p. 161-183.
- Boyd, F.S. and Wolfe, H.D., 1953, Recent investigations of radioactive occurrences in Sierra, Doña Anna, and Hidalgo Counties, New Mexico: New Mexico Geological Society, Guidebook 4, p. 141-142.
- Cathelineau, M., 1986, The hydrothermal alkali metasomatism effects on granitic rocks: quartz dissolution and related subsolidus changes: *Journal of Petrology*, v. 27, p. 945-965.
- Charoy, B. and Pollard, P.J., 1989, Albite-rich, silica-depleted metasomatic rocks at Emuford, northeast Queensland: mineralogical, geochemical, and fluid inclusion constraints on hydrothermal evolution and tin mineralization: *Economic Geology*, v. 84, p. 1850-1874.
- Condie, K.C. and Budding, A.J., 1979, Geology and geochemistry of Precambrian rocks, central and south-central New Mexico: New Mexico Bureau of Mines and Mineral Resources, Memoir 35, 60 p.
- Condomines, M., Loubeau, O., and Patrier, P., 2007, Recent mobilization of U-series radionuclides in the Bernardan U deposit (French Massif Central): *Chemical Geology*, v. 244, p. 304-315.
- Costi, H.T., Dall'Agnol, R., Borges, R.M.K., Minuzzi, O.R.R., and Teixeira, J.T., 2002, Tin-bearing sodic episyenites associated with the Proterozoic, A-type Água Boa Granite, Pitinga mine, Amazonian craton, Brazil: *Gondwana Research*, v. 5, p. 435-451.
- Cuney, M., Emetz, A., Mercadier, J., Mykchaylov, V., Shunko, W., and Yulsenko, A., 2012, Uranium deposits associated with Na-metasomatism from central Ukraine: A review of some of the major deposits and genetic constraints: *Ore Geology Reviews*, v. 44, p. 82-106.
- Deer, W.A., Howie, R.A., and Zussman, J., 1992, *An Introduction to the Rock Forming Minerals*: Hong Kong, Longman Scientific and Technical, v. 2, 696 p.
- Green, G. N. and O'Neill, J. M., eds., 1998, Digital earth science database, Caballo Resource Area, Sierra and Otero Counties, south-central New Mexico: U.S. Geological Survey, Open-file report OF98-780, CD-ROM.
- Hecht, L., Thuro, K., Plinninger, R., and Cuney, M., 1999, Mineralogical and geochemical characteristics of hydrothermal alteration and episyenitization in the Königshain granites, northern Bohemian massif, Germany: *International Journal of Earth Sciences*, v. 88, p. 236-252.
- Kelley, V.C., 1949, *Geology and economics of New Mexico iron ore deposits*: University of New Mexico, Publications in Geology, no. 2, 246 p.



- Kelley, V.C., and Silver, C., 1952, Geology of the Caballo Mountains: New Mexico University of New Mexico, Publications in Geology, no. 4, 286 p.
- LeBas, M.J., 2008, Fenites associated with carbonatites: *Canadian Mineralogist*, v. 46, p. 915-932.
- Leroy, J., 1978, The Margnac and Fanay uranium deposits of the La Crouzille district (western Massif Central, France: Geologic and fluid inclusion studies: *Economic Geology*, v. 73, p. 1611-1634.
- Long, K.R., van Gosen, B.S., Foley, N.K. and Cordier, D., 2010, The principle rare earth elements deposits of the United States—A summary of domestic deposits and a global perspective: U.S. Geological Survey, Scientific Investigations Report 2010-5220, 104 p.
- López-Moro, F.J., Moro, M.C., Timón, S.M., Cembranos, M.L., and Cór, J., 2013, Constraints regarding gold deposition in episyenites: the Permian episyenites associated with the Villalcampo shear zone, central western Spain: *International Journal of Earth Sciences (Geol. Rundsch.)*, v. 102, p. 721-744.
- McLemore, V.T., 1986, Geology, geochemistry, and mineralization of syenites in the Red Hills, southern Caballo Mountains, Sierra County, New Mexico: New Mexico Geological Society, Guidebook 37, p. 151-159.
- McLemore, V.T., 2013, Geology and mineral resources in the Zuni Mountains mining district, Cibola County, New Mexico: Revisited: New Mexico Geological Society, Guidebook 64, p. 131-142.
- McLemore, V.T., 2015, Rare Earth Elements (REE) Deposits in New Mexico: Update: New Mexico Geology, v. 37, p. 59-69.
- McLemore, V.T., 2016, Episyenites in the Sevilleta National Wildlife Refuge, Socorro County, New Mexico—Preliminary Results; Geology of the Belen area: New Mexico Geological Society, Guidebook 67, p. 255-262.
- McLemore, V.T. and Lueth, V., 2017, Metallic Mineral Deposits, in McLemore, V.T., Timmons, S., and Wilks, M., eds., *Energy and Mineral Deposits in New Mexico*: New Mexico Bureau of Geology and Mineral Resources Memoir 50 and New Mexico Geological Society Special Publication 13, 92 p.
- McLemore, V.T., and McKee, C., 1988, Geochemistry of Burro Mountains syenites and adjacent Proterozoic granite and gneiss and the relationship of a Cambrian–Ordovician magmatic event in New Mexico and southern Colorado: New Mexico Geological Society, Guidebook 39, p. 89-98.
- McLemore, V.T. and McKee, C., 1989, Geology and geochemistry of syenites and adjacent Proterozoic granitic and metamorphic rocks in the Zuni Mountains, Cibola County, New Mexico: New Mexico Geological Society, Guidebook 40, p. 149-155.
- McLemore, V.T., McMillan, N.J., Heizler, M., and McKee, C., 1999, Cambrian alkaline rocks at Lobo Hill, Torrance County, New Mexico: More evidence for a Cambrian-Ordovician aulacogen: New Mexico Geological Society, Guidebook 50, p. 247-253.
- McLemore, V.T., Rämö, O.T., Heizler, M.T. and Heinonen, A.P., 2012, Intermittent Proterozoic plutonic magmatism and Neoproterozoic cooling history in the Caballo Mountains, Sierra County, New Mexico; Preliminary Results: New Mexico Geological Society, Guidebook 63, p. 235-248.
- McMillan, N.J. and McLemore, V.T., 2004, Cambrian-Ordovician Magmatism and Extension in New Mexico and Colorado: New Mexico Bureau of Mines and Geology Resources, Bulletin 160, 12 p.
- Melancon, P.E., 1952, Uranium occurrences in the Caballo Mountains, Sierra County, New Mexico: U.S. Atomic Energy Commission, Technical Memorandum 213, 7 p.
- Nakamura, N., 1974, Determination of REE, Ba, Fe, Mg, Na, and K in carbonaceous and ordinary chondrites: *Geochimica et Cosmochimica Acta*, v. 38, p. 757-775.
- Nishimoto, S., Yoshida, H., Asahara, Y., Tsuruta, T., Ishibashi, M., Katsuta, N., 2014, Episyenite formation in the Toki granite, central Japan: Contributions to Mineralogy and Petrology, v. 167, article 960, 12 p.
- Petersson, J. and Eliasson, T., 1997, Mineral evolution and element mobility during episyenitization (dequartzification) and albitization in the post-kinematic Bohus granite, southwest Sweden: *Lithos*, v. 42, p. 123-146.
- Recio, C., Fallick, A.E., Ugidos, J.M., and Stephens, W.E., 1997, Characterization of multiple fluid-granite interaction processes in the episyenites of Avila-Béjar, central Iberian massif, Spain: *Chemical Geology*, v. 143, p. 127-144.
- Riggins, A.M., 2014, Origin of the REE-bearing episyenites in the Caballo and Burro Mountains, New Mexico [M.S. thesis]: Socorro, New Mexico Institute of Mining and Technology, 348 p.
- Riggins, A.M., Dunbar, N., McLemore, V.T., Heizler, M., McIntosh, W. and Frempong, K., 2014, Mineralogy, geochemistry, and chronology of the Caballo and Burro Mountains REE-bearing episyenites (abstr.): Society of Economic Geology: *Building Exploration Capability for the 21<sup>st</sup> Century, Program. (poster)*, [http://geoinfo.nmt.edu/staff/mclemore/projects/documents/Riggins\\_SEG.pdf](http://geoinfo.nmt.edu/staff/mclemore/projects/documents/Riggins_SEG.pdf), accessed 3/30/18.
- Seager, W.R., and Mack, G.H., 1991, Geology of Garfield quadrangle, Sierra and Doña Ana Counties, New Mexico: New Mexico Bureau of Mines and Mineral Resources, Bulletin 128, 24 p.
- Seager, W.R., and Mack, G.H., 2003, Geology of the Caballo Mountains, New Mexico: New Mexico Bureau of Mines and Mineral Resources, Memoir 49, 136 p.
- Seager, W.R., and Mack, G.H., 2005, Geology of Caballo and Apache Gap quadrangles, Sierra County, New Mexico, New Mexico Bureau of Geology and Mineral Resources, Geologic Map 74, scale 1:24,000.
- Smith, A.E., 2018, Multi-stage processes for generation REE-enriched episyenites and fenites in New Mexico and Colorado: the role of magmatic and diagenetic fluids based on <sup>40</sup>Ar/<sup>39</sup>Ar geochronology, whole rock geochemistry and radiogenic isotopes [M.S. thesis]: New Mexico Institute of Mining and Technology, Socorro, in review.
- Staatz, M.H., Adams, J.W., and Conklin, N.M., 1965, Thorium-bearing microcline-rich rocks in the southern Caballo Mountains, Sierra County, New Mexico: U.S. Geological Survey, Professional Paper 525D, p. 48-51.





A view of the Organ Mountains. Photograph by Dana S. Ulmer-Scholle.

Proterozoic	Neo	541			
		1000			
	Meso		crystalline basement: granitic rocks ~1.4 Ga, metamorphic rocks ~1.7-1.6 Ga		
		1600			
	Paleo	2500			
	Cambrian		485	Bliss ss, ls	
	Ordovician		443		
				Montoya dol, ss	
	Silurian		419	Fusselman dol	
	Devonian		359		
				Percha sh	
				Canutillo ls, sh	
	Mississippian		323		
				Helms sh, ls	
				Rancheria ls	
				Lake Valley ls	
				Caballero slt, dol	
	Pennsylvanian		299		
				Bar B ls, sh	
				Nakaye ls, sh	
				Red House ls, sh, ss	
				Lead Camp ls, sh	
				Panther Seep ls, sh, ss	
	Permian		252		
				north Yeso ss, dol, gyp, ls	
				Abo ss, slt, sh	
				Hueco ls, sh, dol, slt	
				upper Abo middle lower	

Late Cretaceous	Maastrichtian	66	McRae	Hall Lake (lower part) cgl, ss, sh, ft 73.2		
	72.1	Jose Creek cgl, ss, sh, ft 74.9				
	Campanian					
	83.6	86.3	Crevasse Canyon ss, sh			
	Santonian					
	Coniacian					
	89.8	Turonian	Gallup ss, sh			
	D-Cross Tongue, Mancos sh, ss					
	Tres Hermanos		Carthage ss, sh			
			Atarque ss			
93.9	Tokay Tongue, Mancos sh, ss, ls, fb					
Cenomanian	Dakota ss, sh					
	100.5	south	Mojado ss, sh	north	Sarten ss, sh	
	Albian	U-Bar ls, ss				
113		Hell-to-Finish cgl, ss, sh				
125						
Neocomian						
						145
						Jurassic
201	Triassic					
		252				

cgl=conglomerate; ss=sandstone; slt=siltstone; ls=limestone; dol=dolostone; gyp=gypsum; fb=fallout tuff or bentonite

Seager (1973, 1981); Seager and Mack (1994, 2003); Karlstrom et al. (2004); Mack (2004); Armstrong et al. (2004); Kues and Giles (2004); Seager et al. (2008); Hook et al. (2012); Amato et al. (2017). Numbers adjacent to stratigraphic units correspond to radioisotopic ages in Ma or Ga.